Kinetic Analysis for the Effect of Intramolecular Hydrogen Bonding on Photophysical Properties of *N*-Hydroxyalkyl-1,8-naphthalimides

Kazuhiko Matsubayashi,[1] Chisato Kajimura,[1] Hideo Shiratori,[1]
Yasuo Kubo,*[1] Toshitada Yoshihara,[2] and Seiji Tobita[2]

[1]Department of Materials Science, Faculty of Science and Engineering, Shimane University, Matsue 690-8504

[2]Department of Chemistry, Gunma University, Kiryu 376-8515

Received December 11, 2009; E-mail: kubo@riko.shimane-u.ac.jp

N-Methyl-, *N*-(2-hydroxyethyl)-, *N*-(2-methoxyethyl)-, *N*-(3-hydroxypropyl)-, and *N*-(3-methoxypropyl)-1,8-naphthalimide (**1**, **2a, 2b**, **3a**, and **3b**, respectively) were prepared and their photophysical properties examined. The UV and IR spectra of **2a** and **3a** in dichloromethane showed the presence of intramolecular hydrogen bonding between the carbonyl group and the hydroxy group. In addition, the fluorescence intensities of **2a** and **3a** in dichloromethane were found to be about two times larger than those of **1**, **2b**, and **3b**. Furthermore, the fluorescence lifetimes of **2a** and **3a**, determined by picosecond single photon counting, were about two times longer than those of **1**, **2b**, and **3b**. The rate constants of the intersystem crossing (k_{isc}) for **2a** and **3a**, calculated based on the quantum yields of the intersystem crossing (Φ_{isc}) determined by the time-resolved thermal lensing technique, were about one half of those obtained for **1**, **2b**, and **3b**, while the rate constants of fluorescence emission (k_{f}) and internal conversion (k_{ic}) were minimally affected by the presence of intramolecular hydrogen bonding. Enhancement of the fluorescence quantum yield and the lifetime of **2a** and **3a** was thus explained by a decrease in the efficiency of the intersystem crossing from $^1(\pi\pi^*)$ to $^3(\mathrm{n}\pi^*)$, that results from an increase in the energy of the $^3(\mathrm{n}\pi^*)$ level due to the presence of intramolecular hydrogen bonding.

Hydrogen bonding in the ground state is known to play an important role in chemistry and biology.[1,2] On the other hand, intermolecular hydrogen bonds formed in the excited state have often been observed to be stronger than those in the ground state due to specific charge localization in the exited state.[3] Strong hydrogen bonding in the excited state has been reported to induce efficient radiationless deactivation, electron transfer,[4,5] and energy transfer.[6] Formation of intermolecular hydrogen bonds has also been found to have a significant influence on the photophysical behavior of various compounds, especially heterocyclic aromatic[7] and carbonyl compounds.[8,9] Formation of hydrogen bonds has been shown to have different effects on the energies of various excited states; in an extreme case, hydrogen bonding caused the reversal of close-lying nπ^* and $\pi\pi^*$ states.[10] In addition, the difference in strength of hydrogen bonding between the ground and the excited states has been reported to lead to efficient energy dissipation.[8,9,11]

Derivatives of 1,8-naphthalimide have been extensively studied in recent decades owing to their interesting photophysical properties[12] and the wide range of applications they find in chemical and biochemical areas. Many naphthalimide chromophores, characterized by both intense absorption and high fluorescence quantum yields, have been prepared in the last century and used as dyes[13] or brighteners.[14] Several 1,8-naphthalimide-containing compounds have been described as photo-inducible DNA-cleaving agents[15] and tumoricidals,[16] some of which have entered clinical trials owing to their strong anticancer activity.[17] The 1,8-naphthalimide moiety has also been used to design fluorescent molecular probes sensitive to variations in pH[18] or metal ion concentration.[19] Meanwhile, the photoreactions of naphthalimides have been investigated in the past decade by Kubo and co-workers.[20]

We have recently shown that the fluorescence intensity and photoreactivity of *N*-methyl-1,8-naphthalimide (**1**) are remarkably increased by intermolecular hydrogen bonding with alcohols, possibly through a decrease in the efficiency of intersystem crossing from $^1(\pi\pi^*)$ to $^3(\mathrm{n}\pi^*)$, because the energy of the $^3(\mathrm{n}\pi^*)$ level increases as a result of the hydrogen bonding.[21] In this paper, we report the photophysical properties of *N*-methyl-, *N*-(2-hydroxyethyl)-, *N*-(2-methoxyethyl)-, *N*-(3-hydroxypropyl)-, and *N*-(3-methoxypropyl)-1,8-naphthalimide (**1**, **2a**, **2b**, **3a**, and **3b**, respectively; Scheme 1) to clarify the mechanistic details of the effect of hydrogen bonding on the photophysical properties of naphthalimide derivatives.

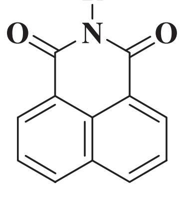

1 ; R = Me
2a ; R = $(CH_2)_2OH$
2b ; R = $(CH_2)_2OMe$
3a ; R = $(CH_2)_3OH$
3b ; R = $(CH_2)_3OMe$

Scheme 1.

Published on the web August 21, 2010; doi:10.1246/bcsj.20090330

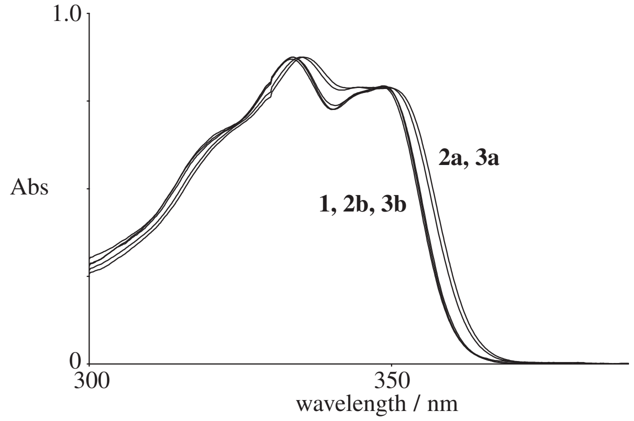

Figure 1. UV spectra of naphthalimides **1**–**3** (0.075 mM) in dichloromethane.

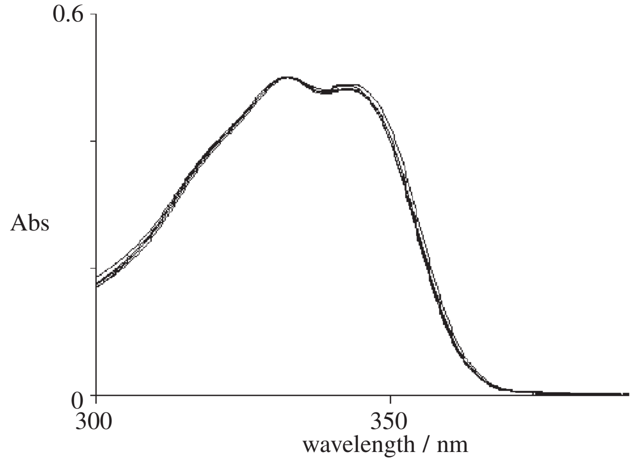

Figure 2. UV spectra of naphthalimides **1**–**3** (0.060 mM) in methanol.

Results and Discussion

UV and IR Spectra. To prove the existence of intramolecular hydrogen bonding in the ground state, UV absorption spectra of **2a** and **3a** in dichloromethane were measured together with those of **1**, **2b**, and **3b** (Figure 1). The absorption spectra of **2a** and **3a** were found to be clearly red-shifted compared with those of **1**, **2b**, and **3b**, which were indistinguishable. These results indicate the presence of intramoleculer hydrogen bonding in **2a** and **3a**.

In methanol, however, the absorption spectra of compounds **1**–**3** were indistinguishable. It is possible that the intramolecular hydrogen bonding in **2a** and **3a** is disrupted by the polar protic solvent (Figure 2).

IR spectra of **2a** and **3a** in dichloromethane were measured together with those of **1**, **2b**, and **3b** (Figure 3). Figure 3 shows the slight red-shift and broadening of the intense absorption bands attributed to the νC=O of **2a** and **3a**. These results further indicate the formation of hydrogen bonds between the carbonyl group and the intramolecular hydroxy group in **2a** and **3a**.

DFT Calculations. To elucidate the nature of the intramolecular hydrogen bonds in the ground states of **2a** and **3a**, DFT calculations (geometry optimizations) for these compounds at the RB3LYP[22]/6-31+G(d) level were examined using the Gaussian 03 package.[23] The calculations indicate that the hydrogen bonding geometries (HB form) are more stable than the corresponding non-hydrogen bonding geometries (non-HB form) for **2a** and **3a** (Figures 4 and 5, respectively). These results further support the presence of intramolecuar hydrogen bonding in **2a** and **3a**.

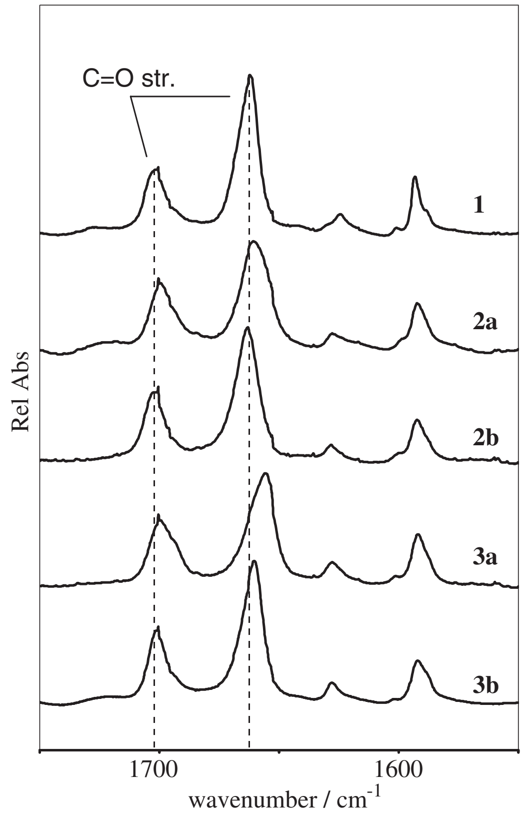

Figure 3. IR spectra of the νC=O region of naphthalimides **1**–**3** (20 mM) in dichloromethane.

Fluorescence Spectra. To confirm that intramolecular hydrogen bonding has an effect on ^{1}**2a*** and ^{1}**3a***, fluorescence spectra of **2a** and **3a** in dichloromethane were measured together with those of **1**, **2b**, and **3b**. Figure 6 shows that the fluorescence intensities of **2a** and **3a** are about two times larger than those of **1**, **2b**, and **3b**.

In methanol, however, the fluorescence spectra of compounds **1**–**3** showed no clear systematic variations; the relative fluorescence intensities of **1**, **2a**, **2b**, **3a**, and **3b** were 1.00, 0.80, 0.90, 1.08, and 0.87, respectively.

Fluorescence Quantum Yields and Lifetimes. The fluorescence decay profiles for compounds **1**–**3** were measured by the picosecond single photon counting method. Typical fluorescence decay profiles for **1** and **2a** in dichloromethane are shown in Figure 7 and the lifetimes (τ_f) of ^{1}**1*** and ^{1}**2a*** were determined to be 180 and 371 ps, respectively. The fluorescence quantum yield (Φ_f) values for **1**–**3** in dichloromethane were determined as relative values to those obtained for **1** in acetonitrile ($\Phi_f = 0.027$).[12] The values for τ_f and Φ_f of compounds **1**–**3** in dichloromethane at ambient temperature

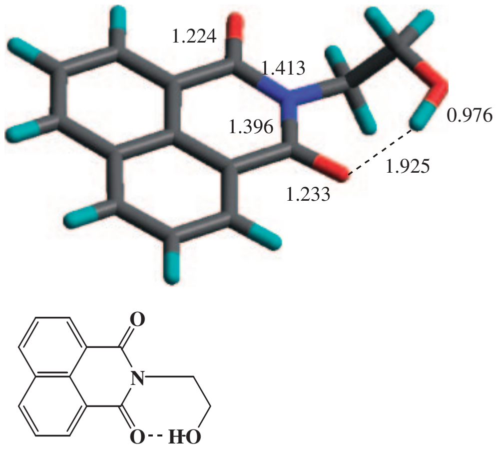

2a
HB form

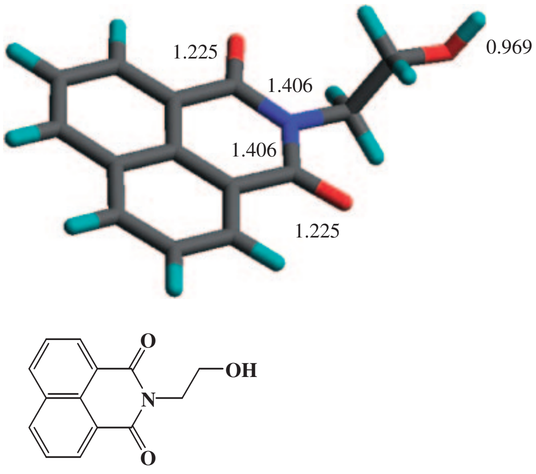

2a
non-HB form

Figure 4. Optimized hydrogen bonding geometry (HB form, total energy = $-262.91533\,\text{kcal mol}^{-1}$) and non-hydrogen bonding geometry (non-HB form, total energy = $-262.72322\,\text{kcal mol}^{-1}$) for naphthalimide **2a** calculated using RB3LYP/6-31+G(d) (lengths in Å).

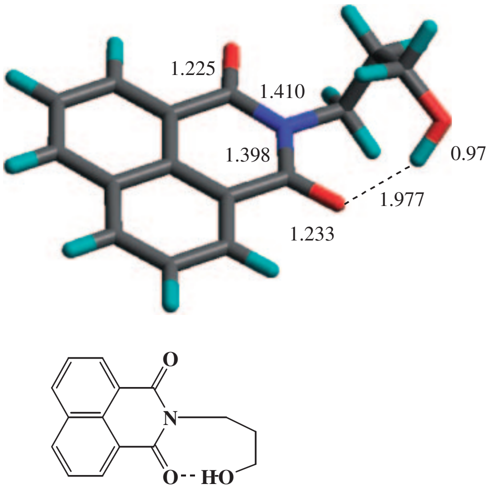

3a
HB form

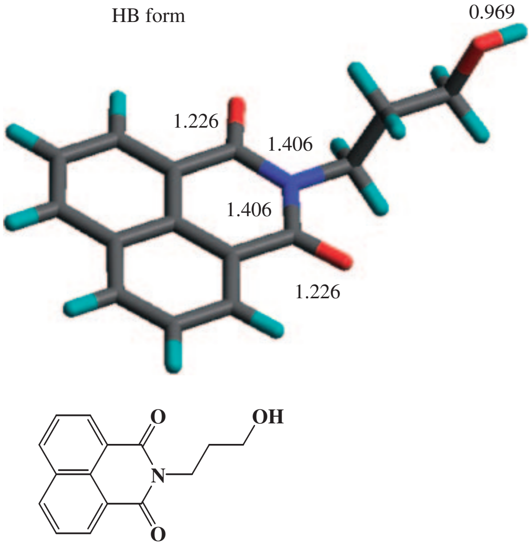

3a
non-HB form

Figure 5. Optimized hydrogen bonding geometry (HB form, total energy = $-287.32382\,\text{kcal mol}^{-1}$) and non-hydrogen bonding geometry (non-HB form, total energy = $-286.80799\,\text{kcal mol}^{-1}$) for naphthalimides **3a** calculated using RB3LYP/6-31+G(d) (lengths in Å).

are summarized in Table 1. It can be seen that both the τ_f and Φ_f values for **2a** and **3a**, in which the intramolecular hydrogen bond is formed, are about two times greater than those obtained for **1**, **2b**, and **3b**.

Quantum Yields and Rate Constants. To establish the cause of the increase in τ_f and Φ_f values for **2a** and **3a**, the quantum yields for intersystem crossing (Φ_isc) in compounds **1**–**3** were determined by using the time-resolved thermal lensing (TRTL) method.[24] Typical TRTL signals for **1** and **2a** in dichloromethane are shown in Figure 8.

The ratio $U_\mathrm{slow}/U_\mathrm{total}$ of the intensity of the slow rise component (U_slow) and that of the total TRTL signal (U_total) is given by:

$$\frac{U_\mathrm{slow}}{U_\mathrm{total}} = \frac{\Phi_\mathrm{isc} E_\mathrm{T}}{E_\mathrm{ex} - \Phi_\mathrm{f}\langle E_\mathrm{s}\rangle} \tag{1}$$

where E_T, E_ex, and $\langle E_\mathrm{s}\rangle$ are the 0–0 transition energy of ^{3}**1**–**3***, the excitation photon energy (80.5 kcal mol^{-1}, 28170 cm^{-1}) and the average energy dissipated by fluorescence from ^{1}**1**–**3***, respectively. The E_T value of **1** was determined to be 52.9 kcal mol^{-1} from the 0–0 band of the phosphorescence spectrum of **1** in EPA at 77 K, and the $\langle E_\mathrm{s}\rangle$ value of **1** was determined to be 75.64 kcal mol^{-1} from the wavelength of the maximum intensity of the fluorescence of **1** in dichloromethane. The slow rise component for **1**, which corresponds to the slow thermal release from ^{3}**1***, was slightly larger than that for **2a**. The Φ_isc values of **1** and **2a** were estimated by eq 1, and the Φ_ic value was calculated by:

$$\Phi_\mathrm{ic} = 1 - \Phi_\mathrm{f} - \Phi_\mathrm{isc} \tag{2}$$

The values of the quantum yields Φ_f, Φ_isc, and Φ_ic for compounds **1**–**3** are also included in Table 1.

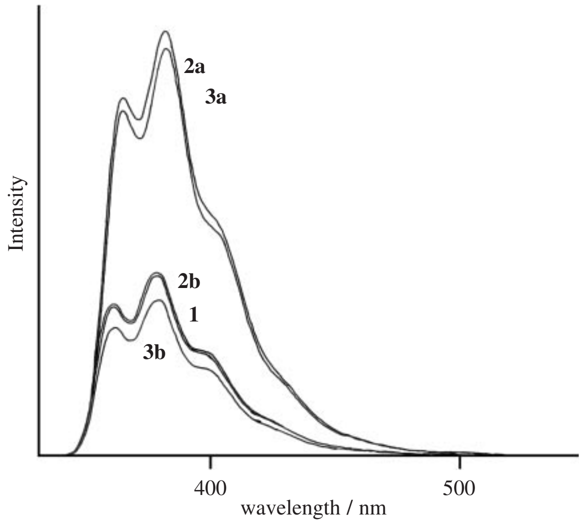

Figure 6. Fluorescence spectra of naphthalimides **1**–**3** (0.075 mM) in dichloromethane.

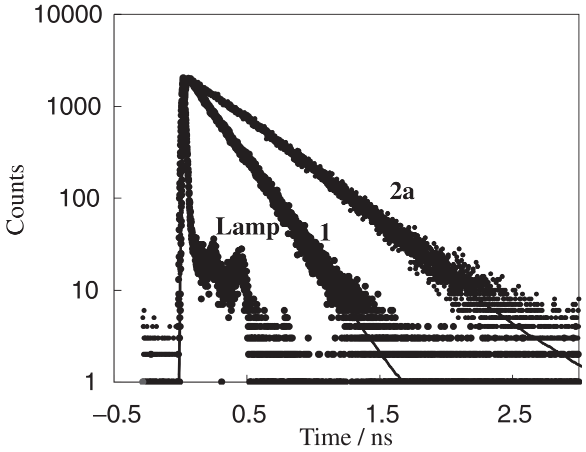

Figure 7. Fluorescence decay curves of naphthalimides **1** and **2a** (0.022 mM) in dichloromethane.

Table 1. Photophysical Parameters of Naphthalimides **1**–**3** in Dichloromethane

Imide	τ_f /ps	Φ_f	Φ_{isc}[a]	Φ_{ic}	k_f /10^8 s^{-1}	k_{isc} /10^9 s^{-1}	k_{ic} /10^8 s^{-1}	$k_q\tau$ /M^{-1}	k_q /10^{10} M^{-1} s^{-1}
1	180	0.030	0.92	0.05	1.7	5.1	2.8	2.89	1.62
2a	371	0.060	0.85	0.09	1.6	2.3	2.4	5.37	1.45
2b	172	0.029	0.91	0.06	1.7	5.3	3.5	2.54	1.48
3a	358	0.057	0.86	0.08	1.6	2.4	2.2	5.46	1.52
3b	141	0.023	0.94	0.04	1.6	6.7	2.8	2.18	1.55

a) The Φ_{isc} values determined using the TRTL method.

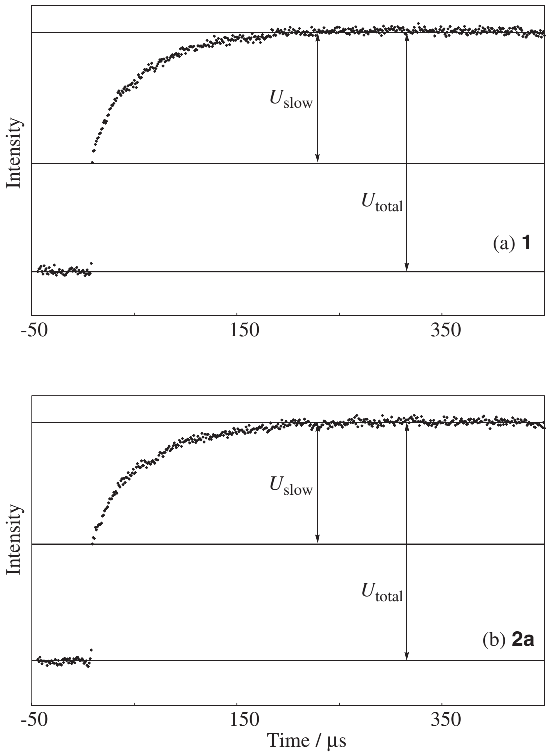

Figure 8. Time-resolved thermal lensing signals of naphthalimides **1** and **2a** (0.022 mM) in dichloromethane.

The rate constants for fluorescence emission (k_f), intersystem crossing (k_{isc}), and internal conversion (k_{ic}) for compounds **1**–**3** were calculated by substituting the values determined for Φ_f, Φ_{isc}, Φ_{ic}, and τ_f into eqs 3, 4, and 5, respectively:

$$k_f = \Phi_f {\tau_f}^{-1} \tag{3}$$

$$k_{isc} = \Phi_{isc} {\tau_f}^{-1} \tag{4}$$

$$k_{ic} = \Phi_{ic} {\tau_f}^{-1} \tag{5}$$

The values of k_f, k_{isc}, and k_{ic} for compounds **1**–**3** in dichloromethane at ambient temperature are also presented in Table 1. It can be seen in the table that the values for k_{isc} ($\approx 10^9$ s^{-1}) are significantly larger than those for k_f ($\approx 10^8$ s^{-1}) and k_{ic} ($\approx 10^8$ s^{-1}) for all of the compounds in dichloromethane, indicating that the intersystem crossing is the most dominant relaxation process ($\Phi_{isc} > 0.85$) from ^{1}**1**–**3***. Furthermore, the k_{isc} values for **2a** and **3a** decrease to about one half of the values obtained for the other naphthalimides. In the cases of k_f and k_{ic}, minimal differences were observed. Thus, the intramolecular hydrogen bonding in **2a** and **3a** may only affect the rate of intersystem crossing (k_{isc}).

Fluorescence Quenching. The fluorescence of compounds **1**–**3** was quenched by the presence of styrene in dichloromethane without any change in the shape or wavelength of the maximum emission. Typical examples for **1** and **2a** are shown in Figure 9. Stern–Volmer plots for the fluorescence quenching gave straight lines against the concentration of styrene. The

Stern–Volmer slopes ($k_q\tau_f$) and rate constants for fluorescence quenching (k_q) for compounds **1**–**3** are summarized in Table 1 as well. While the values of $k_q\tau_f$ for **2a** and **3a** are about two times larger than those obtained for the other naphthalimides, the rate constants of the fluorescence quenching (k_q) for **2a** and **3a** are comparable to the diffusion-controlled rate constant in dichloromethane and almost identical to those of **1**, **2b**, and **3b**, indicating that the intramolecular hydrogen bonding has very little effect on the rate of fluorescence quenching by styrene.

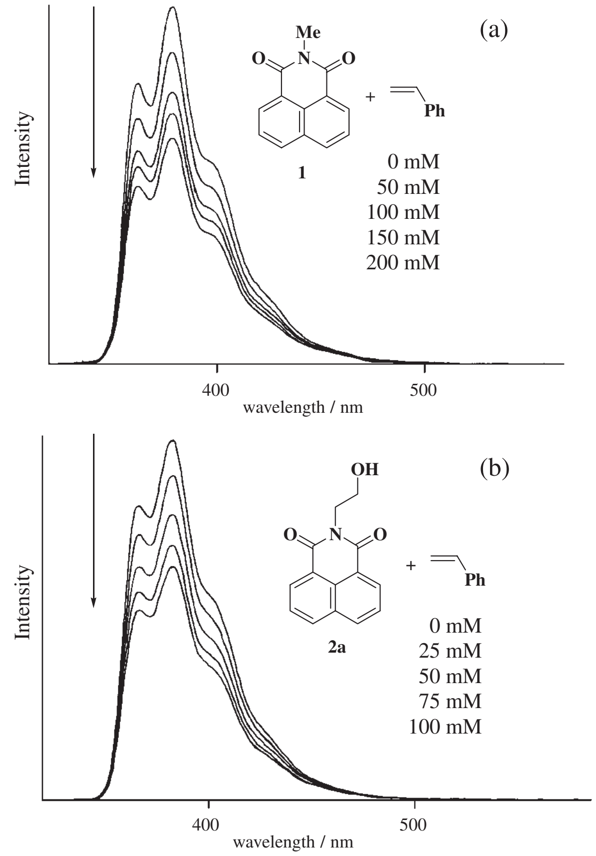

Figure 9. Fluorescence spectra of naphthalimides **1** and **2a** (0.075 mM) in the presence of styrene at various concentrations in dichloromethane.

Mechanism. As shown above, intersystem crossing in **1** accounts for more than 85% of the relaxation process of ^{1}**1***. The results may indicate that the lowest singlet excited state $^1(\pi\pi^*)$ and the upper triplet excited state $^3(n\pi^*)$ levels of **1** are close together in energy.

On the other hand, fluorescence quantum yields (Φ_f) for **2a** and **3a** increased due to the presence of intramolecular hydrogen bonding. Hydrogen bond formation is known to increase the energy of the $n\pi^*$ state compared with that of the $\pi\pi^*$ state.[25] The $^1(\pi\pi^*)$ and $^3(n\pi^*)$ levels in **2a** and **3a** are close together in energy, but intramolecular hydrogen bonding in these two naphthalimides may increase the energy of the $^3(n\pi^*)$ compared with that of the $^1(\pi\pi^*)$, thus decreasing the rate of intersystem crossing from the $^1(\pi\pi^*)$ to the $^3(n\pi^*)$ level and resulting in an increase in the fluorescence quantum yield (Φ_f) (Scheme 2).

Conclusion

Prezhdo et al. have reported that the ability of *N*-hydroxyalkyl-1,8-naphthalimides to form intramolecular hydrogen bonds depends on the number of OH groups, and that the introduction of a single OH group does not increase the fluorescence quantum yield.[26] Thus, only *N*-(1,1-dihydroxymethyl-2-hydroxy)ethyl-1,8-naphthalimide (**4**) (Chart 1) with three OH groups was shown to exhibit an increase in the fluorescence quantum yield as a result of intramoleclar hydrogen bond formation.

On the contrary, our results clearly indicate that the introduction of only one hydroxy group into the *N*-alkyl side

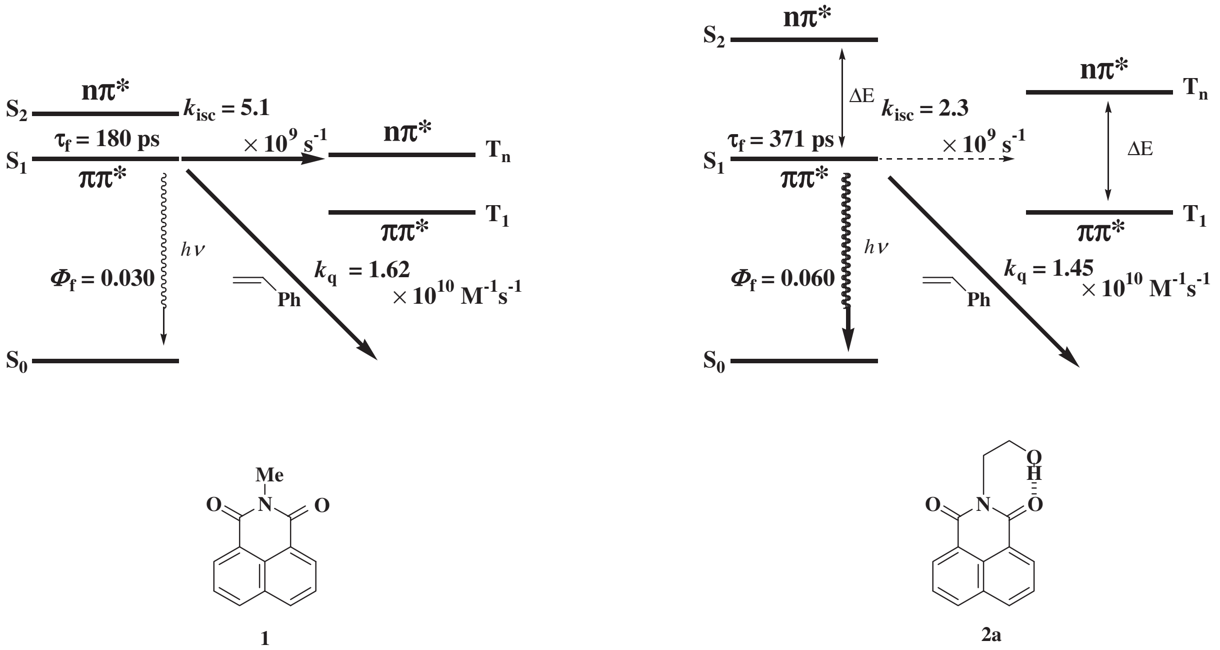

Scheme 2.

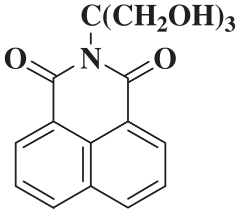

4

Chart 1. Structural formula of **4**.

chain increases the fluorescence quantum yield of 1,8-naphthalimides about two times. The ability to markedly control the photophysical properties and photoreactivities of 1,8-naphthalimide derivatives with the simple introduction of a single intramolecular hydrogen bond may be of significant interest given that naphthalimides are widely used in numerous applications.

Experimental

General. UV spectra were measured by use of a JASCO UVIDEC-650 spectrometer. Fluorescence spectra were obtained on a Hitachi 850 spectrophotometer. Melting points were obtained on a Yanagimoto micro melting point apparatus and are uncorrected. NMR spectra were recorded on a JEOL JNM-AL-400 (400 MHz) instrument. Chemical shifts are reported in ppm (δ) relative to an internal standard ($SiMe_4$). IR spectra were obtained using a JASCO FT/IR-350 spectrometer. Mass spectra (EI, 70 eV) were recorded on a Hitachi M-80B mass spectrometer. Combustion analyses were performed on a Yanagimoto CHN corder MT-5.

The picosecond lifetime measurements were carried out by using a self-mode-locked Ti:sapphire laser (center wavelength 800 nm, pulse width ca. 70 fs, repetition rate 82 MHz) pumped by a Nd^{3+}:YAG laser (532 nm, 4.5 W). The generation of the second harmonic (400 nm, pulse width ca. 200 fs) was performed in a lithium triborate (LBO) crystal. The third harmonic (266 nm, pulse width ca. 250 fs) was generated by a sum frequency mixing of the fundamental and the second harmonic. The repetition frequency of the excitation pulse was reduced to 4 MHz by using a pulse picker. The second harmonic (400 nm) in the output beam was used as trigger pulse. The fluorescence from the sample solution was observed through a polarizer at the magic angle (54.7°) with respect to the polarization direction of the excitation laser pulse. The emission light was detected by a microchannel plate after passing through a monochromator. The instrument response function had a half-width of 20–25 ps. Analysis of the fluorescence decay curves was carried out using the deconvolution method.

The quantum yields for intersystem crossing (Φ_{isc}) in naphthalimides were determined by means of the time-resolved thermal lensing (TRTL) method. For TRTL measurements, the third harmonic (355 nm) of a nanosecond Nd^{3+}:YAG laser (pulse width 6 ns) was utilized for the excitation source. A He-Ne laser beam (633 nm) was used as the monitoring light. The probe light was introduced into a monochromator after passing through an optical filter and a small pinhole (300 µm diameter). The intensity change of the probe beam was detected by a photomultiplier. The TRTL signals were recorded on a digitizing oscilloscope and were averaged over five hundred laser shots to improve the signal-to-noise ratio. The absorbance of the sample solutions for the TRTL measurements was adjusted to ca. 0.10 at the excitation wavelength. The TRTL experiments were carried out at 293 K.

The equilibrium geometries of **2a** and **3a** were optimized by DFT calculations by using the B3LYP[22] functional and 6-31+G(d) basis set. Total energies were evaluated by using 6-311+G(d,p) basis set, and corrected with zero point vibration energies. All theoretical calculations were carried out on Gaussian 03 package.[23]

Materials. *N*-Methyl-1,8-naphthalimide (**1**) was prepared according to the published procedure.[27] Solvents and styrene were commercially available.

***N*-(2-Hydroxyethyl)-1,8-naphthalimide (2a):** Naphthalimide **2a** was prepared from 2-aminoethanol (15 mL, 250 mmol) and 1,8-naphthalic anhydride (20 g, 100 mmol) according to the procedure reported for **1**. Recrystallization of the crude material from methanol gave 24 g (99 mmol) of **2a** in 99% yield as colorless columns. Mp 177.0–178.0 °C. ^{1}H NMR ($CDCl_3$): δ 2.38 (t, $J = 5.6$ Hz, 1H), 3.99 (dt, $J = 5.4$, 5.6 Hz, 2H), 4.47 (t, $J = 5.4$ Hz, 2H), 7.77 (dd, $J = 7.3$, 8.3 Hz, 2H), 8.23 (d, $J = 8.3$ Hz, 2H), 8.61 (d, $J = 7.3$ Hz, 2H). ^{13}C NMR ($CDCl_3$): δ 42.8 (CH_2), 61.9 (CH_2), 122.4 (C), 127.0 (CH), 128.2 (C), 131.5 (CH), 131.6 (C), 134.2 (CH), 165.1 (C=O). IR (KBr): 3484, 1698, 1655, 1588, 1380, 1348, 1323, 1235, 1032, 778 cm^{-1}. MS (70 eV): m/z 241 (M^+, 10), 222 (12), 210 (68), 198 (100), 180 (72), 152 (61), 126 (83). Found: C, 70.02; H, 4.80; N, 5.95%. Calcd for $C_{14}H_{11}NO_3$: C, 69.70; H, 4.60; N, 5.81%.

***N*-(2-Methoxyethyl)-1,8-naphthalimide (2b):** To a methanol solution (100 mL) of **2a** (6.8 g, 28 mmol) was added sulfuric acid (8.0 mL), followed by refluxing for 8 h. The solution was then poured into 300 mL of water and the precipitate filtered. Recrystallization of the crude material from methanol gave 0.43 g (1.7 mmol) of **2b** in 6% yield as colorless columns. Mp 124.0–125.0 °C. ^{1}H NMR ($CDCl_3$): δ 3.39 (s, 3H), 3.74 (t, $J = 5.9$ Hz, 2H), 4.46 (t, $J = 5.9$ Hz, 2H), 7.75 (dd, $J = 7.3$, 8.5 Hz, 2H), 8.22 (d, $J = 8.5$ Hz, 2H), 8.62 (d, $J = 7.3$ Hz, 2H). ^{13}C NMR ($CDCl_3$): δ 39.0 (CH_2), 58.6 (CH_3), 69.5 (CH_2), 122.3 (C), 126.6 (CH), 127.8 (C), 131.0 (CH), 131.3 (C), 133.6 (CH), 163.9 (C=O). IR (KBr): 1698, 1658, 1591, 1438, 1376, 1359, 1235, 1120, 1046, 783 cm^{-1}. MS (70 eV): m/z 255 (M^+, 85), 223 (80), 210 (89), 197 (42), 180 (89), 152 (92), 126 (100). Found: C, 70.71; H, 5.30; N, 5.59%. Calcd for $C_{15}H_{13}NO_3$: C, 70.58; H, 5.13; N, 5.49%.

***N*-(3-Hydroxypropyl)-1,8-naphthalimide (3a):** Naphthalimide **3a** was prepared from *n*-propanolamine (45 mL, 590 mmol) and 1,8-naphthalic anhydride (60 g, 300 mmol). Recrystallization of the crude material from methanol gave 54 g (300 mmol) of **3a** in a quantitative yield as colorless needles. Mp 123.0–124.0 °C. ^{1}H NMR ($CDCl_3$): δ 2.00 (m, 2H), 3.15 (t, $J = 6.9$ Hz, 1H), 3.59 (dt, $J = 6.1$, 6.9 Hz, 2H), 4.36 (t, $J = 6.1$ Hz, 2H), 7.78 (dd, $J = 7.3$, 8.3 Hz, 2H), 8.24 (d, $J = 8.3$ Hz, 2H), 8.63 (d, $J = 7.3$ Hz, 2H). ^{13}C NMR ($CDCl_3$): δ 30.9 (CH_2), 36.7 (CH_2), 58.8 (CH_2), 122.2 (C), 126.9 (CH), 128.1 (C), 131.5 (C), 131.5 (CH), 134.2 (CH), 164.7 (C=O).

IR (KBr): 3435, 1695, 1644, 1620, 1591, 1346, 1245, 1173, 923, 785 cm^{-1}. MS (70 eV): *m/z* 255 (M^+, 72), 222 (72), 211 (92), 197 (45), 180 (84), 152 (86), 126 (100). Found: C, 70.77; H, 5.25; N, 5.61%. Calcd for $C_{15}H_{13}NO_3$: C, 70.58; H, 5.13; N, 5.49%.

***N*-(3-Methoxypropyl)-1,8-naphthalimide (3b):** To a methanol solution (300 mL) of **3a** (8.0 g, 31 mmol) was added sulfuric acid (20 mL), followed by refluxing for 24 h. The solution was then poured into 300 mL of water and the precipitate filtered. Recrystallization of the crude material from methanol gave 3.7 g (14 mmol) of **3b** in 44% yield as colorless cubics. Mp 100.0–101.0 °C. ^{1}H NMR ($CDCl_3$): δ 2.03 (m, 2H), 3.34 (s, 3H), 3.53 (t, $J = 6.6$ Hz, 2H), 4.29 (t, $J = 6.6$ Hz, 2H), 7.75 (dd, $J = 7.1$, 8.5 Hz, 2H), 8.21 (d, $J = 8.5$ Hz, 2H), 8.61 (d, $J = 7.1$ Hz, 2H). ^{13}C NMR ($CDCl_3$): δ 28.1 (CH_2), 37.7 (CH_2), 58.4 (CH_3), 70.5 (CH_2), 122.5 (C), 126.7 (CH), 127.9 (C), 130.9 (CH), 131.4 (C), 133.6 (CH), 163.8 (C=O). IR (KBr): 1696, 1657, 1626, 1589, 1443, 1344, 1233, 1116, 906, 783 cm^{-1}. MS (70 eV): *m/z* 269 (M^+, 41), 222 (42), 211 (79), 198 (100), 180 (65), 152 (64), 126 (65). Found: C, 71.42; H, 5.78; N, 5.33%. Calcd for $C_{16}H_{15}NO_3$: C, 71.36; H, 5.61; N, 5.20%.

Supporting Information

Parameters of the coordinates of optimized geometries of **2a** and **3a**. This material is available free of charge on the web at: http://www.csj.jp/journals/bcsj/.

References

1 C. F. Mellot, A. M. Davidson, J. Eckert, A. K. Cheetham, *J. Phys. Chem. B* **1998**, *102*, 2530.

2 G. A. Jeffrey, W. Saenger, *Hydrogen Bonding in Biological Structures*, Springer-Verlag, Berlin, **1991**.

3 M. Sugita, T. Shimada, H. Tachibana, H. Inoue, *Phys. Chem. Chem. Phys.* **2001**, *3*, 2012.

4 H. Miyasaka, A. Tabata, S. Ojima, N. Ikeda, N. Mataga, *J. Phys. Chem.* **1993**, *97*, 8222.

5 H. Miyasaka, A. Tabata, K. Kamada, N. Mataga, *J. Am. Chem. Soc.* **1993**, *115*, 7335.

6 J. L. Sessler, B. Wang, A. Harriman, *J. Am. Chem. Soc.* **1995**, *117*, 704.

7 J. Herbich, C.-Y. Hung, R. P. Thummel, J. Waluk, *J. Am. Chem. Soc.* **1996**, *118*, 3508, and references therin.

8 L. Biczók, T. Bérces, H. Linschitz, *J. Am. Chem. Soc.* **1997**, *119*, 11071.

9 a) T. Yatsuhashi, H. Inoue, *J. Phys. Chem. A* **1997**, *101*, 8166. b) T. Yatsuhashi, Y. Nakajima, T. Shimada, H. Tachibana, H. Inoue, *J. Phys. Chem. A* **1998**, *102*, 8657, and references therein.

10 M. J. van der Burgt, L. M. G. Jansen, A. H. Huizer, C. A. G. O. Varma, *Chem. Phys.* **1995**, *201*, 525.

11 a) A. Sinicropi, W. M. Nau, M. Olivucci, *Photochem. Photobiol. Sci.* **2002**, *1*, 537. b) J. Waluk, *Acc. Chem. Res.* **2003**, *36*, 832.

12 V. Wintgens, P. Valat, J. Kossanyi, L. Biczok, A. Demeter, T. Bérces, *J. Chem. Soc., Faraday Trans.* **1994**, *90*, 411.

13 E. Martin, R. Weigand, A. Pardo, *J. Lumin.* **1996**, *68*, 157.

14 I. Grabtchev, T. Philipova, *Dyes Pigm.* **1995**, *27*, 321.

15 W. Yao, X. Qian, Q. Hu, *Tetrahedron Lett.* **2000**, *41*, 7711.

16 M. F. Braña, J. M. Castellano, M. Morán, M. J. Pérez de Vega, X. D. Qian, C. A. Romerdahl, G. Keilhauer, *Eur. J. Med. Chem.* **1995**, *30*, 235.

17 P. F. Bousquet, M. F. Braña, D. Conlon, K. M. Fitzgerald, D. Perron, C. Cocchiaro, R. Miller, M. Moran, J. George, X. D. Qian, G. Keilhauer, C. A. Romerdahl, *Cancer Res.* **1995**, *55*, 1176.

18 L. M. Daffy, A. P. de Silva, H. Q. N. Gunaratne, C. Huber, P. L. M. Lynch, T. Werner, O. Wolfbeis, *Chem.—Eur. J.* **1998**, *4*, 1810.

19 B. Ramachandram, G. Saroja, N. B. Sankaran, A. Samanta, *J. Phys. Chem. B* **2000**, *104*, 11824.

20 Y. Kubo, M. Suto, S. Tojo, T. Araki, *J. Chem. Soc., Perkin Trans. 1* **1986**, 771.

21 K. Matsubayashi, Y. Kubo, *J. Org. Chem.* **2008**, *73*, 4915.

22 a) A. D. Becke, *J. Chem. Phys.* **1993**, *98*, 5648. b) C. Lee, W. Yang, R. G. Parr, *Phys. Rev. B* **1988**, *37*, 785. c) P. J. Stephens, F. J. Devlin, C. F. Chabalowski, M. J. Frisch, *J. Phys. Chem.* **1994**, *98*, 11623.

23 M. J. Frisch, G. W. Trucks, H. B. Schlegel, G. E. Scuseria, M. A. Robb, J. R. Cheeseman, G. Scalmani, V. Barone, B. Mennucci, G. A. Petersson, H. Nakatsuji, M. Caricato, X. Li, H. P. Hratchian, A. F. Izmaylov, J. Bloino, G. Zheng, J. L. Sonnenberg, M. Hada, M. Ehara, K. Toyota, R. Fukuda, J. Hasegawa, M. Ishida, T. Nakajima, Y. Honda, O. Kitao, H. Nakai, T. Vreven, J. A. Montgomery, Jr., J. E. Peralta, F. Ogliaro, M. Bearpark, J. J. Heyd, E. Brothers, K. N. Kudin, V. N. Staroverov, R. Kobayashi, J. Normand, K. Raghavachari, A. Rendell, J. C. Burant, S. S. Iyengar, J. Tomasi, M. Cossi, N. Rega, J. M. Millam, M. Klene, J. E. Knox, J. B. Cross, V. Bakken, C. Adamo, J. Jaramillo, R. Gomperts, R. E. Stratmann, O. Yazyev, A. J. Austin, R. Cammi, C. Pomelli, J. W. Ochterski, R. L. Martin, K. Morokuma, V. G. Zakrzewski, G. A. Voth, P. Salvador, J. J. Dannenberg, S. Dapprich, A. D. Daniels, O. Farkas, J. B. Foresman, J. V. Ortiz, J. Cioslowski, D. J. Fox, *Gaussian 03, Revision D.02*, Gaussian, Inc., Wallingford, CT, **2004**.

24 T. Yoshihara, H. Shimada, H. Shizuka, S. Tobita, *Phys. Chem. Chem. Phys.* **2001**, *3*, 4972.

25 G. J. Brealey, M. Kasha, *J. Am. Chem. Soc.* **1955**, *77*, 4462.

26 O. V. Prezhdo, B. V. Uspenskii, V. V. Prezhdo, W. Boszczyk, V. B. Distanov, *Dyes Pigm.* **2007**, *72*, 42.

27 C. Somich, P. H. Mazzocchi, H. L. Ammon, *J. Org. Chem.* **1987**, *52*, 3614.